RSC Advances

ROYAL SOCIETY OF CHEMISTRY

www.rsc.org/advances

Paper written as a *communication* for submission to *RSC Advances*

Carbonaceous Multiscale-Cellular Foams as Novel Electrodes for Stable Efficient Lithium-Sulfur Batteries

Martin Depardieu,[1,3] Raphaël Janot,[2] Clément Sanchez,[3] Ahmed Bentaleb,[1] Christel Gervais,[3] Marc Birot,[4] Rezan Demir-Cakan[2,5], Rénal Backov[1,] and Mathieu Morcrette[2,*]*

[1] Université de Bordeaux, Centre de Recherche Paul Pascal, UPR 8641 CNRS, 115 Avenue Albert Schweitzer, 33600 Pessac, France.

Email : backov@crpp-bordeaux.cnrs.fr

[2] Laboratoire de Réactivité et Chimie des Solides, UMR 7314 CNRS, Université de Picardie Jules Verne, 33 Rue Saint Leu, 80039 Amiens, France / / Réseau sur le Stockage Electrochimique de l'Energie (RS2E), FR CNRS 3459, France

Email : mathieu.morcrette@u-picardie.fr

[3] Sorbonne Universités, UPMC Univ Paris 06, CNRS, Collège de France, UMR 7574, Chimie de la Matière Condensée de Paris, F-75005, Paris, France.

[4] Université de Bordeaux, Institut des Sciences Moléculaires, UMR 5255 CNRS, 351 cours de la Libération, 33405 Talence, France

[5,] Gebze Institute of Technology, Department of Chemical Engineering, 41400 Gebze, Turkey

Abstract

Porous carbon foams were prepared by pyrolysis of phenolic resin from a dual template approach, using silica monoliths as hard templates and triblock copolymers as soft templating agents. Macroporosity of 50-80% arose from the Si(HIPE) hard template, while the soft template generated micro- or mesoporosity, according to the operating procedure. The final materials exhibit BET specific surface areas of 400-900 $m^2 \cdot g^{-1}$, depending on the use or not of non-ionic surfactant during the synthetic paths. Their performances as Li-sulfide battery positive electrodes were investigated. The novel 2P5HF carbon foam presents more than 800 $mA \cdot h \cdot g^{-1}$ (150 $mA \cdot h \cdot cm^{-3}$) of remnant capacity after 50 cycles, an unprecedented performance.

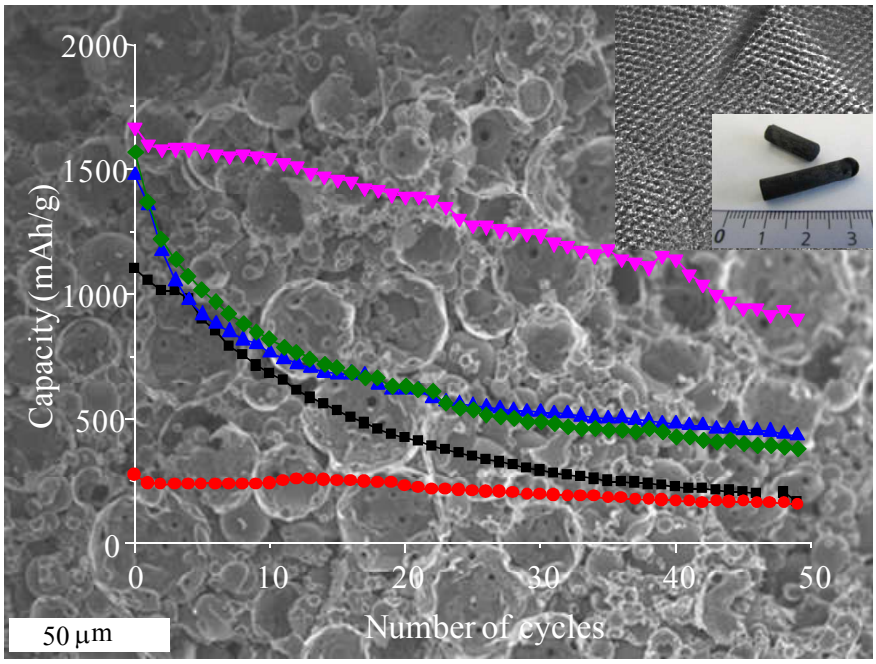

Keywords: Porous carbon; HIPE; Li-Sulfide battery; Integrative chemistry; Energy

Introduction

Due to a unique set of specificities (high surface area, large pore volume, chemical inertness addressed through good mechanical stability, good conductivity) open cell carbonaceous materials appear as outstanding candidates for a wide scope of applications ranging from water and air purification, adsorption, electro-catalysis and energy storage and conversion.[1,2] The rational design of such porous carbonaceous materials is thus of first importance and relies either on hard or soft templating synthetic paths where pore morphologies, pore sizes and size distributions are tuned with a certain versatility. The hard template route[3] is based on pre-existing hard porous templates impregnated with a carbon source being subsequently carbonized under non-oxidative atmosphere. After dissolution of the hard template, a negative carbonaceous replica is finally obtained. Ordered mesoporous carbons (OMC) have been reported through insertion of carbon precursors within mesoporous silica particles.[4] In this field, various hard templates have been chosen according to their nature like alumina membranes[5] or zeolites,[6] or to their porous structures characteristics like silica-based MCM-48,[7] SBA-15,[4c] MSU-H[8] and MSU-1.[9] More complex architectures can also be obtained using bimodal[9,10] zirconia-based parallel macrochannels,[11] or colloidal crystal templating[12] OMC materials. Particularly, for increasing the easy shape process and continuity of physical properties at high scale in combination with mass transport optimization, there is a crucial need for monolith-type carbonaceous materials bearing hierarchical porosity.[13] In this context, we have proposed recently generation of carbonaceous micro-macroporous[14a] and meso-macroporous[14b] monolithic foams using silica-HIPE[15] as exo-templating matrices, HIPE being the acronym for High Internal Phase Emulsion.[16]

Li-ion battery devices have been extensively used as the primary electrical energy storage devices in several lightweight portable electronics. Despite this fact, the current Li-ion battery technology does not meet the high energy and high power densities for larger

applications such as electric vehicles (EVs). The main penalty relies on intrinsic cathode chemistry using transition metal compounds to store electrical energy which induces a theoretical limit to the current Li-ion batteries and therefore prevents to reach the goal of driving EVs on Li-ion batteries. Lithium-sulfur chemistry holds great promise for achieving the goal of EV battery applications with a theoretical capacity of 1675 $mA{\cdot}h{\cdot}g^{-1}$, nearly one magnitude higher than that of $LiFePO_4$ cathodes (theoretical capacity 176 $mA{\cdot}h{\cdot}g^{-1}$).[17] Nevertheless, the Li/S system has not been implemented in EVs because of several issues that still need being circumvented, as the dissolution of sulfur that reacts with lithium metal induces a non stable SEI layer and the insulating character of sulfur and Li_2S irreversibly deposit both at the cathode and Li anode.[18] One way of optimizing both charge transport while constraining polysulfides at the cathode is their confinement within conductive carbonaceous porous media,[19] while more recently, an original path employing *in situ* chemically synthesized polysulfide species, leading to liquid-based cathodes labeled "catholytes", have shown to generate superior performances than conventional Li-S cell configuration.[20] They demonstrate the key role of the strength and porosity of the carbon electrode into the electrochemical properties and the detrimental formation of Li_2S at the porous carbon matrix. In the present study, we decided to assess Li/S batteries capacity using carbonaceous foams bearing tunable porosity and try to correlate the obtained capacity with the macrocellular foams porosity and surface area.

Experimental section

Chemicals

Tetraethoxysilane ($Si(OEt)_4$, TEOS), purity >99 %; dodecane, purity >90 %; block copolymers Synperonic® P123 and Pluronic® F127 (poly(ethylene glycol)-block-poly(propylene glycol)-block-poly(ethylene glycol)) were purchased from Aldrich.

Cetyltrimethylammonium bromide ($(C_{16}H_{33})N(CH_3)_3Br$, CTAB), purity 98 %, was purchased from ChemPur. Hydrochloric acid, 37 %, was purchased from Carlo Erba Reagents. Ablaphene RS101 (formophenolic prepolymer resin of the resol type in a hydroalcoholic solution) was purchased from Rhodia. All chemicals were used as received without further purification.

Macrocellular silica hard template synthesis (Si-HIPE)

The silica hard template is a typical Si-HIPE, which synthesis from the combination of sol-gel chemistry and a concentrated emulsion has already been studied and described elsewhere.[15] Typically, TEOS (5 g) is added to an acidified concentrated CTAB solution (16 g of 35 wt% CTAB in water with 6 g HCl). The solution is hand stirred until it becomes clear as the TEOS is hydrolyzed. The solution is then poured into a mortar and dodecane (35 g) is added drop by drop while stirring slowly with a pestle. After the last drop of dodecane, stirring is maintained for a few seconds to ensure the absence of visible dodecane drops in the concentrated emulsion and its homogeneity. This emulsion is then poured into moulds – in this case polystyrene test tubes – and is left to rest for a week while the condensation reactions take place. Drying at this stage is to be avoided, so the tubes are either closed or put under a saturated water/ethanol atmosphere. After condensation, the samples are put in a 1:1 THF/acetone mix three times for 24 h to eliminate dodecane. They are then slowly dried in a desiccator over a few days. After drying, the Si-HIPE are calcinated at 650 °C for 6 h with a heating rate of 2 °C/min and a first plateau at 200 °C for 2 h to eliminate surfactant residues.

Porous carbon foams synthesis

The overall foams synthetic paths are described elsewhere.[14] Typically, Si-HIPE monoliths are immerged in a beaker containing a solution composed of either: 25 wt%

phenolic resin in THF (25HF); 80 wt% phenolic resin in THF (80HF); a 15:2:5 mix of ethanol, P123 and phenolic resin (2P5HF); a 15:4:5 mix of ethanol, F127 and phenolic resin (4F5HF). The beakers are placed under a dynamic vacuum until the end of the effervescence due to the air removal from the silica foams. The system is then let under static vacuum for three days. The samples are rapidly rinsed with THF and then placed at 80 °C for 24 h into an oven to initiate resin polymerization. To complete the polymerization, a thermal treatment in air at 155 °C for 5 h is applied with a heating rate of 2 °C·min^{-1} with a first plateau at 80 °C for 12 h followed by a second one at 110 °C for 3 h. Pyrolysis is performed at 900 °C for 1 h, with a heating rate of 4 °C·min^{-1}. A plateau at 350 °C for 30 min is added for samples 2P5HF and 4F5HF to ensure copolymers elimination before pyrolysis. Silica hard templates are removed by washing the samples with a 10 v% HF solution for 24 h, which is eliminated by rinsing three times for 24 h in distilled water.

Characterizations

SEM observations were performed with a Hitachi TM-1000 apparatus at 15 kV. The specimens were gold-palladium-coated in a vacuum evaporator prior to examination. High-resolution TEM (HR-TEM) micrographs were obtained with a Jeol 2200 FS microscope. The samples were prepared as follows: carbonaceous powders were deposited on a copper grid coated with a Formvar/carbon membrane. Surface areas and pore characteristics on micro/mesoscales were obtained with a Micromeritics ASAP 2010 apparatus. Intrusion/extrusion mercury measurements were performed using a Micromeritics Autopore IV porosimeter, this to reach the macrocellular scaffolds characteristics.

Electrochemical tests

Electrolyte solution used in this study was 1 M lithium bis(trifluoromethanesulfonyl)imide (LiTFSI) containing tetramethylene sulfone (TMS). Li_2S_6 was chemically synthesized by reacting stoichiometric amounts of sulfur and lithium in ethylene glycol diethyl ether at 150 °C. A precise amount of active material Li_2S_6 was dissolved in the electrolyte leading to the final concentration of 1M of Li_2S_6 and caution has been taken to introduce a very precise quantity of electrolyte. Carbon foams were very smoothly grinded in order to keep the porosity without any added carbons. Galvanostatic and potentionstatic cycling measurements are performed with a classical two-electrode Swagelok-type™ cell using 0.1 mL electrolyte with C/10 current densities voltage range between 1.0-3.0 V *vs*. Li with VMP3 (Bio-logic, France).

Results and discussion

On a macroscopic length scale, as obtained before,[14] the carbonaceous foams obtained from Si(HIPE) as a hard template are in a self-standing monolithic state, bearing open porosity with a texture that resembles aggregated hollow spheres (Figure 1). More quantitative information is obtained through mercury porosimetry measurements (Table 1). We can notice that the porosity percentage is roughly inversely proportional to the weight percentage of resin employed during the synthetic routes. As such, 80HF sample is bearing the lower porosity percentage when compared with the other three foams.

Table 1. Foams macroscopic characteristics extracted from mercury porosimetry.

Materials	Starting wt% resin in THF	Intrusion volume ($cm^3 \cdot g^{-1}$)	Porosity (%)	Bulk density ($g \cdot cm^{-3}$)	Skeletal density ($g \cdot cm^{-3}$)
80HF	80	0.7	49	0.70	1.36
25HF	25	5.6	82	0.15	0.82
2P5HF	23	6.7	83	0.12	0.72
4F5HF	21	5.2	76	0.15	0.62

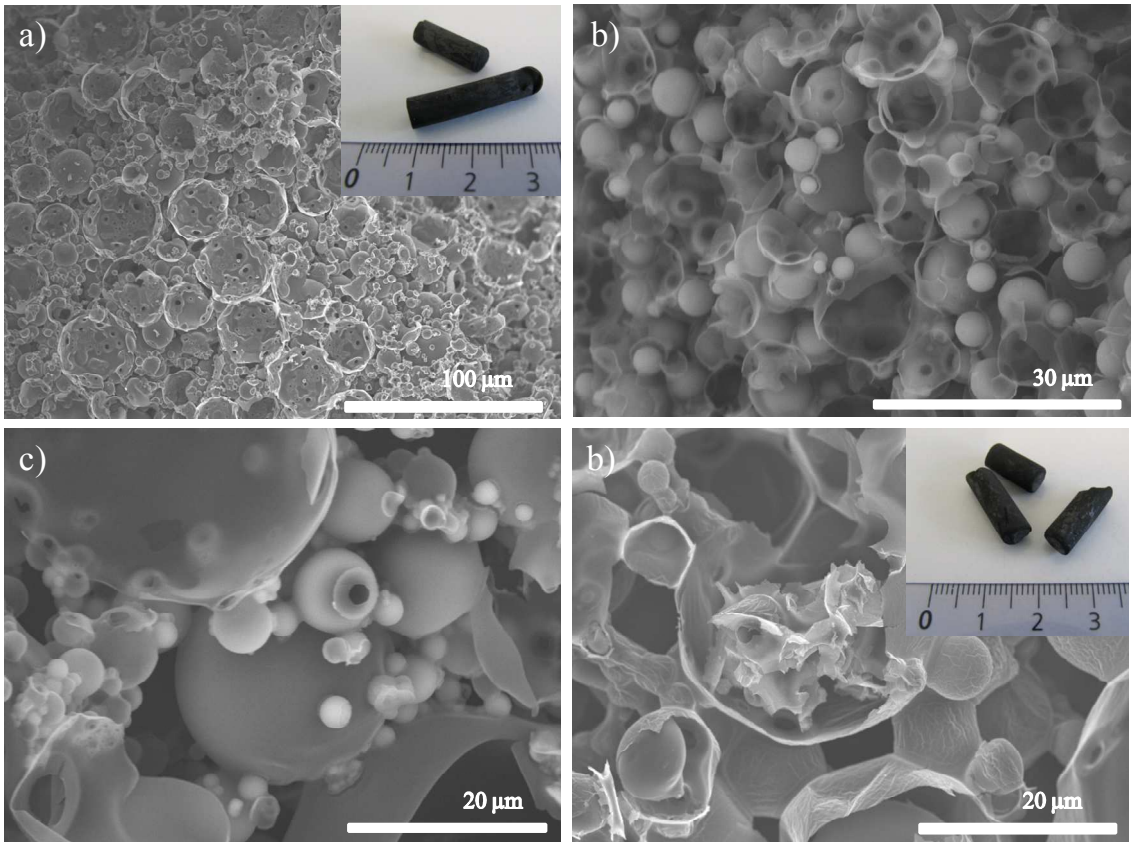

Figure 1. SEM micrographs of the macrocellular carbonaceous foams. a) 80HF, b), 2P5HF c), 25HF d) 4F5HF. Embedded optical pictures show the monolithic character of the foams.

In the same trend, the bulk density is also inversely proportional to the starting amount of resin. Considering the skeleton density, we can notice that it decreases from 80HF to 25HF, as micro/mesoporosity is increased for 25HF (see Table 2). The skeleton density of the carbonaceous foams synthesized with non-ionic surfactant-based mesophases (to increase mesoporosity) is, as expected, decreased further for 2P5HF and 4F5HF monoliths.

Considering the quantitative evaluation of the foams micro/mesoporosity addressed through nitrogen physisorption measurements, the results are summarized within the Table 2. We can see clearly that the use of non-ionic surfactant during the synthetic paths enhanced the mesoscopic surface area by almost 50%. The adsorption-desorption curves (see Figure S1) of 25HF and 80HF are typical of class I, with and abrupt raise at low relative pressure, followed by a plateau, whereas they are typical of mixed class I and IV for 2P5HF and 4F5HF**.** Considering 25HF and 80HF, we can notice that the former is bearing a higher micropores surface area than the latter. This feature is indeed expected, as 25HF is synthesized with 75 wt% of THF (thus 25 wt% of resin), the THF evaporation causing the microporosity, while 80HF is obtained with only 20 wt% of THF (80% of resin). In agreement with its lowest skeleton density (Table 1) 4F5HF exhibits the highest mesopores surface area around 650 $m^2 \cdot g^{-1}$ even when compared with 580 $m^2 \cdot g^{-1}$ for 2P5HF (Table 2). The mesoscopic voids of the foams obtained with the use of non ionic surfactant can be observed through TEM investigations, as proposed within the shown on Figure 2. We can notice that quite organized hexagonal mesoscopic voids are observed for 4F5HF foams, while a less organized vermicular texture is present in 2P5HF.

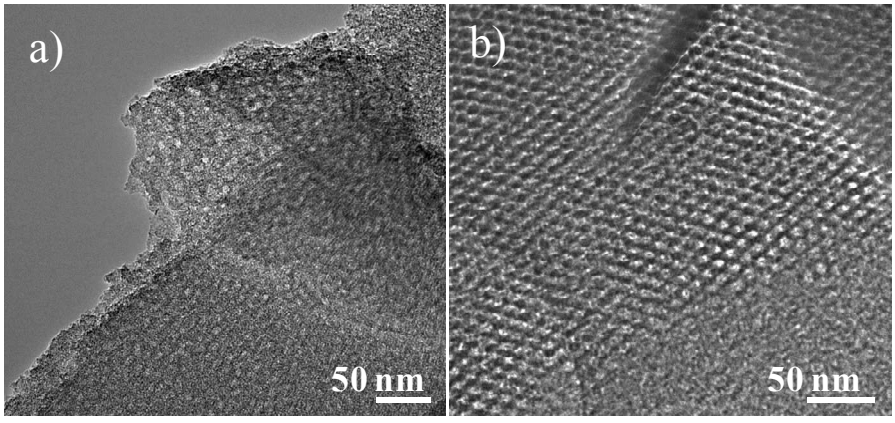

Figure 2. TEM investigations of the multiscale-cellular foams, a) 2P5HF, b) 4F5HF.

The electrochemical cycling of the different carbon foams are shown in Figure 3. At first glance, the results are quite promising for some materials, since we obtained 2 electrons exchanged without any optimization of the electrode, a result close to the theoretical capacity of active sulfur, except 80HF that delivers only 0.4 Li corresponding to 20% of the theoretical capacity. From its foam macroscopic and mesoscopic characteristics, this carbon is the less porous, with still 50% of porosity. The presence of microporous walls in 80HF can explain these poor performances due to problems of electrolyte spreading into the carbon walls inducing thereby two major penalties. One is the presence of less active surface for the oxidation/reduction of polysulfides and the second is the possibility of micropores clogging by the formation of large Li_2S particles. Using the same preparation method, we decided to increase the porosity but keeping the same micro-mesoscopic pore size. 25HF foam presents a macroporosity of 82%, so significantly higher than 80HF foam's one. It is really interesting to see that we were able to exchange 1.2 Li per atom of S (Figure 3). For both cases we can notice that the number of Li exchanged decreased upon cycling : this capacity fading is related to a problem of Li_2S oxidation as more and more lithium seems to be trapped into the electrode at the end of the charge.

Table 2. Foams mesoscopic characteristics extracted from nitrogen physisorption measurements (see SI for nitrogen physisorption curves Figure S1).

Materials	BET surface area ($m^2 \cdot g^{-1}$)	Total pore volume ($cm^3 \cdot g^{-1}$)	*t*-plot surface area ($m^2 \cdot g^{-1}$)		
			External	Mesopores	Micropores
80HF	459	0.20	3	456	
25HF	802	0.37	21	781	
2P5HF	854	0.76	63	581	210
4F5HF	911	0.92	77	653	181

From the capacity retention of the different foams (Figure 4), we want to stress that after 50 cycles, the capacity of 25HF is equal to the one of 80HF, showing a quite good cyclability of 80HF. It can be related to: 1) the poor amount of Li_2S onto the carbon foams, meaning that we can expect a good electronic contact between carbon and non-conducting Li_2S and 2), the high bulk and skeletal densities that can support the volume expansion occurring during the electrochemical process keeping the electrode cohesion.

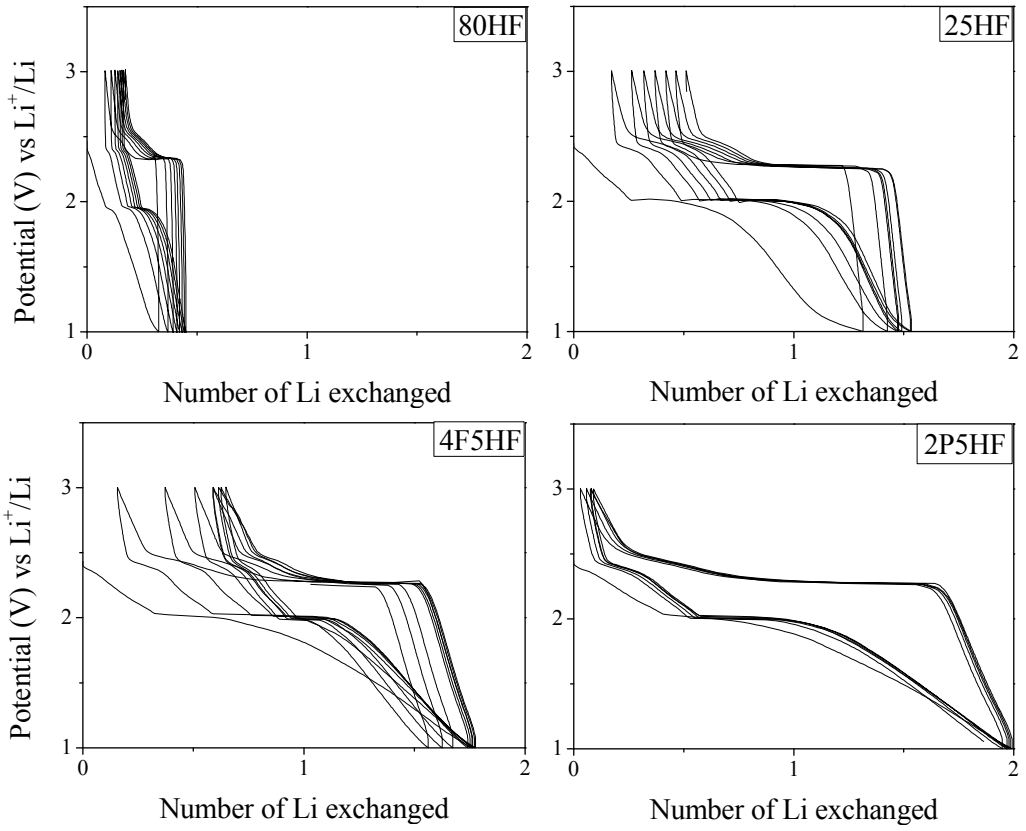

Figure 3. Charge-discharge profiles of Li_2S_6 1M in TMS with different carbon foams *vs*. Li exchanged.

The electrochemical performances of macro/meso/microporous 4F5HF foam are significantly improved compared with 25HF one. 1.7 Li can be inserted during the first discharge and a better reversibility is observed. It is interesting to note that the difference in terms of Li exchanged is not in the number of Li during the different plateau at 2 V and

above, but more in the sloping decrease of the potential at the end of discharge. In terms of porosity, 4F5HF carbon is more porous than 25HF foam. A lower efficiency of the electrochemical reaction would therefore be expected but on the other hand, the porosity in 4F5HF foam is falling in a different size range. We measured 180 $m^2 \cdot g^{-1}$ for microporosity and 650 $m^2 \cdot g^{-1}$ for mesoporosity in 4F5HF to be compared with 780 $m^2 \cdot g^{-1}$ for in between meso/microporosity in 25HF. Mesoporosity seems therefore to be a crucial point for both electrochemical process, especially at end of discharge and for the capacity retention.

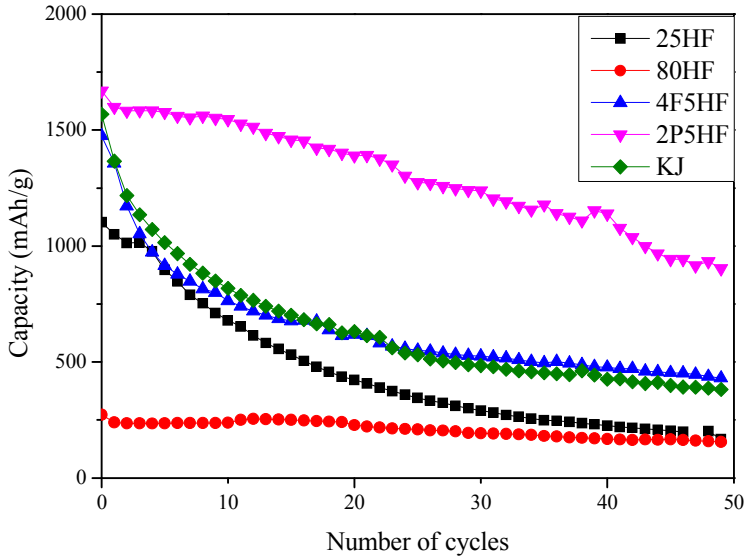

Figure 4. Evolution of the capacity as a function of cycle number with the different carbonaceous foams. KJ stand for commercial microporous Kejten Black carbon (600m^2 g^{-1}).

As such, after 50 cycles, we have measured a capacity of 430 $mA \cdot h \cdot g^{-1}$ for 4F5HF, whereas only 165 $mA \cdot h \cdot g^{-1}$ for 25HF and 80HF. It is interesting to note that the intrusion volume is lower for 4F5HF compared with 25HF, and even worse for 80HF. Maybe this means that we do not have yet a good access for the electrolyte inside the porosity. Moreover, the skeletal density is lower for 4F5HF than for 25HF, so it can explain the poor capacity retention of 4F5HF despite the good reversibility in the first cycles.

In order to merge all the positive aspects presented for the above three compounds, we have tried to synthesize a highly porous carbon foam with micro/mesoporosity while still

bearing high skeletal density into 2P5HF foam. As depicted within Figure 3, the electrochemical properties of 2P5HF are quite impressive, as almost 2 Li are exchanged during the first discharge with a very nice reversibility. All the different cycles perfectly superimposed the previous ones, suggesting excellent capacity retention. This capacity retention can be seen in Figure 4: after 50 cycles 2P5HF presents more than 1000 $mA{\cdot}h{\cdot}g^{-1}$, far above all the other electrodes seen in the literature, within the limit of our knowledge in this domain of energy conversion. Indeed, regarding all the above-mentioned factors that govern the remnant capacity – high surfaces promoted by mesoporosity while preserving as far as it can be a good bulk density (optimizing the active mass per volume) – we can say that 2P5HF foam is offering a quite good compromise between these two needed but antagonist criteria of competence.

As such, if the above results look very interesting when compared to the literature, dealing with porous matter, it seems important to normalize the remnant capacity of those foams, after 50 cycles, with the foams bulk density, providing thereby volumetric capacities rather than mass ones. Doing so, the remnant capacities after 50 cycles, expressed in $mA{\cdot}h{\cdot}cm^{-3}$ are 115, 23, 52 and 150 respectively for the 80HF, 25HF, 4F5HF and 2P5HF porous carbon foams. Again, under this expression of the volumetric remnant capacity we can see that 2P5HF is still bearing the highest efficiency, but the difference with 80HF is less pronounced using this dimensionality. We believe that, dealing with porous media, capacity dimensionality should be proposed both in $mA{\cdot}h{\cdot}g^{-1}$ and also in $mA{\cdot}h{\cdot}cm^{-3}$ in order to be more comparable to one system with another, providing thus absolute comparisons rather than relative ones.

Conclusion

Porous carbon foams were prepared by pyrolysis of phenolic resin from a dual template approach, using silica monoliths as hard templates and triblock copolymers as soft templating agents. Macroporosity of 50-80 % arose from the Si(HIPE) hard template, while soft templates generated micro- or mesoporosity, according to the operating procedure. The final materials exhibited BET specific surface areas of 400-900 $m^2 \cdot g^{-1}$, depending on whether or not non ionic surfactants were used during the synthetic paths. Their performances as Li-sulfide battery negative electrodes were investigated and correlated with their hierarchical porosity. Triggering the porosity through an integrative chemistry-based rational design,[21] we found out that the novel 2P5HF carbon foam presents more than 1000 $mA \cdot h \cdot g^{-1}$ of remnant capacity after 50 cycles, far from all the other electrodes seen in the literature, within the limit of our knowledge. Indeed, regarding all the above-mentioned factors that govern the remnant capacity, high surface area is promoted by mesoporosity while preserving as far as it can be a good bulk density, optimizing thereby the active mass per volume. We can say that the 2P5HF is offering a quite good compromise between these two needed but antagonist criteria of competence where both massic and volumetric capacities have been up-graded.

Reference

1 Foley, H.C. *Microporous Mater*. 1995, *4*, 407.

2 Kyotani, T. *Carbon* 2000, *38*, 269.

3 Schüth, F. *Angew. Chem. Int. Ed*. 2003, *42*, 3604.

4 (*a*) Ryoo, R.; Joo, S.H.; Jun, S. *J. Phys. Chem. B*, 1999, *103*, 7743. (*b*) Lee, J.; Yoon, S.; Hyeon, T.; Oh, S.M.; Kim, K.B. *Chem. Commun.* 1999, 2177. (*c*) Jun, S.; Joo, H.S.; Ryoo, R.; Kruk, M.; Jaroniec, M.; Liu, Z.; Ohsuna, T.; Terasaki, O. *J. Amer. Chem. Soc.* 2000, *122*, 10712. (*d*) Yoon, S.B.; Kim, J.Y.; Yu, J.-S. *Chem. Commun.* 2001, 559.

5 (*a*) Che, G.; Lakshmi, B.B.; Fisher, E.R.; Martin, C.R. *Nature* 1998, *393*, 346. (*b*) Kyotani, T.; Tsai, L.; Tomita, A. *Chem. Mater*. 1995, *7*, 1427.

6 (*a*) Kyotani, T.; Tsai, L.; Inoue, S.; Tomita, A. *Chem. Mater*. 1997, *9*, 609. (*b*) Ma, Z.; Kyotani, T.; Tomita, A. *Chem. Commun*. 2000, 2365. (*c*) Ma, Z.; Kyotani, T.; Tomita, A. *Chem. Mater*. 2001, *13*, 4413.

7 (*a*) Kruk, M.; Jaroniec, M.; Ryoo, R.; Joo, S.H. *J. Phys. Chem. B* 2000, *104*, 7960. (*b*) Joo, S.H.; Jun, S.; Ryoo, R. *Microporous Mesoporous Mater*. 2001, *44-45*, 153. (*c*) Joo, S.H.; Choi, S.J.; Oh, I.; Kwak, J.; Liu, Z.; Terasaki, O; Ryoo, R. *Nature* 2001, *412*, 169.

8 Kim, S.S.; Pinnavaia, T.S. *Chem. Commun*. 2001, 2418.

9 Alvarez, S.; Fuertes, A.B. *Carbon* 2004, *42*, 433.

10 (*a*) Lu, A.-H.; Schmidt, W.; Spliethoff, B.; Schüth, F. *Adv. Mater*. 2003, *15*, 1602. (*b*) Lu, A.-H.; Kiefer, A.; Schmidt, W.; Schüth, F. *Chem. Mater*. 2004, *16*, 100. (*c*) Lu, A.-H.; Li, C.W.; Schmidt, W.; Kiefer, W.; Schüth, F. *Carbon* 2004, *42*, 2939. (*d*) Lee, J.; Kim, J.; Yheon, T. *Chem. Commun*. 2003, 1138. (e) Miyake, T.; Hanaya, M. *J. Mater. Sci*. 2002, *37*, 907. (f) Lee, H.I.; Pak, C.; Shin, C.-H.; Chang, H.; Seung, D.; Yie, J.A. Kim, J.M. *Chem. Commun*. 2005, 6035.

11 Su, B.-L.; Vantomme, A.; Surahy, L.; Pirard, R.; Pirard, J.-P. *Chem. Mater*. 2007, *19*, 3325.

12 Holland, B.T.; Blanford, C.F.; Stein, A. *Science* 1998, *281*, 538.

13 (a) Fan, L.-Z.; Hu, Y.-S.; Maier, J.; Adelhelm, P.; Smarsly, B.; Antonietti, M. *Adv. Funct. Mater*. 2007, *17*, 3083. (b) Hu; Y.-S; Adelhelm, P.; Smarsly; B.M.; Hore, S.; Antonietti, M.; Maier, J. *Adv. Funct. Mater*. 2007, *17*, 1873.

14 *(a)* Brun, N.; Prabaharan, S.R.S.; Morcrette, M.; Sanchez, C.; Pécastaing, G.; Derré, A.; Soum, A.; Deleuze, H.; Birot, M.; Backov, R. *Adv. Funct. Mater*, 2009, *19,* 3136. *(b)* Brun, N.; Prabaharan, S.R.S.; Morcrette, M.; Deleuze, H.; Birot, M.; Babot, O.; Achard, M.-F.; Surcin, C.; Backov, R. *J. Phys. Chem. C*, 2012, *116*, 1408.

15 Carn, F.; Colin, A.; Achard, M.-F.; Deleuze, H.; Birot, M.; Backov, R. *J. Mater. Chem.* 2004, *14*, 1370.

16 (*a*) Barby, D.; Haq, Z. *Eur. Pat.* 0060138, 1982. (*b*) Cameron, N.R.; Sherrington, D.C. in "High Internal Phase Emulsions (HIPEs) Structure, properties and use in polymer preparation" *Advances in Polymer Science*, Eds Springer Berlin / Heidelberg, 1996, *126*, 163. (*b*) Cameron, N. *Polymer* 2005, *46*, 1439. (*c*) Zhang, H.; Cooper, A.I. *Soft Matter* 2005, *2*, 107.

17 (*a*) Akridge, J.R.; Mikhaylik, Y.V.; White, N. *Solid State Ionics* 2004, *175*, 243. (*b*) Cheon, S.E.; Choi, S.S.; Han, J.S.; Choi, Y.S.; Jung, B.H.; Lim, H.S. *J. Electrochem. Soc.* 2004, *151*, A2067. (*c*) Yamin, H.; Gorenshtein, A.; Penciner, J.; Sternberg, Y.; Peled, E. *J. Electrochem. Soc.* 1988, *135*, 1045. (*d*) Kang, K.; Meng, Y.S.; Breger, J.; Grey, C.P.; Ceder, G. *Science* 2006, *311*, 977.

18 (*a*) Herbert, D.; Ulam, J. US pat, N° 3043896, 1962. (b) Elazari, R.; Salitra, G.; Taylosef, Y.; Grinblat, J.; Scordilis-kellay, C.; Xiao, A.; Affinito, J.; Aurbach, D. *J. Electrochem. Soc.* 2010, *157*, A1131.

19 (*a*) Ji, X.; Lee, K.T.; Nazar, L. F. *Nature Mater*. 2009, *8*, 500. (*b*) Wang, H.; Yang, Y.; Liang, Y.; Robinson, J.T.; Li, Y.; Jackson, A.; Gui, Y.; Dai, Y. *Nanolett*. 2011, 2644. (c) Evers, S.; Yim, T.; Nazar, L. F. *J. Phys. Chem.* C 2012, *116*, 19653.

20 Demir-Cakan, R.; Morcrette, M.; Guéguen, A.; Dedryvère, R.; Tarascon, J.-M. *Energy Environ. Sci.* 2013, *6*, 176.

21 (*a*) Backov, R. *Soft Mater* 2006, *2*, 452. (*b*) Brun, N.; Ungureanu, S.; Deleuze, H.; Backov, R.; *Chem. Soc. Rev.*, 2011, *40* , 771. (*c*) Sanchez, C.; Belleville, P.; Popall, M.; Nicole, L. *Chem. Soc. Rev*. 2011, *40*, 696.

Supplemental

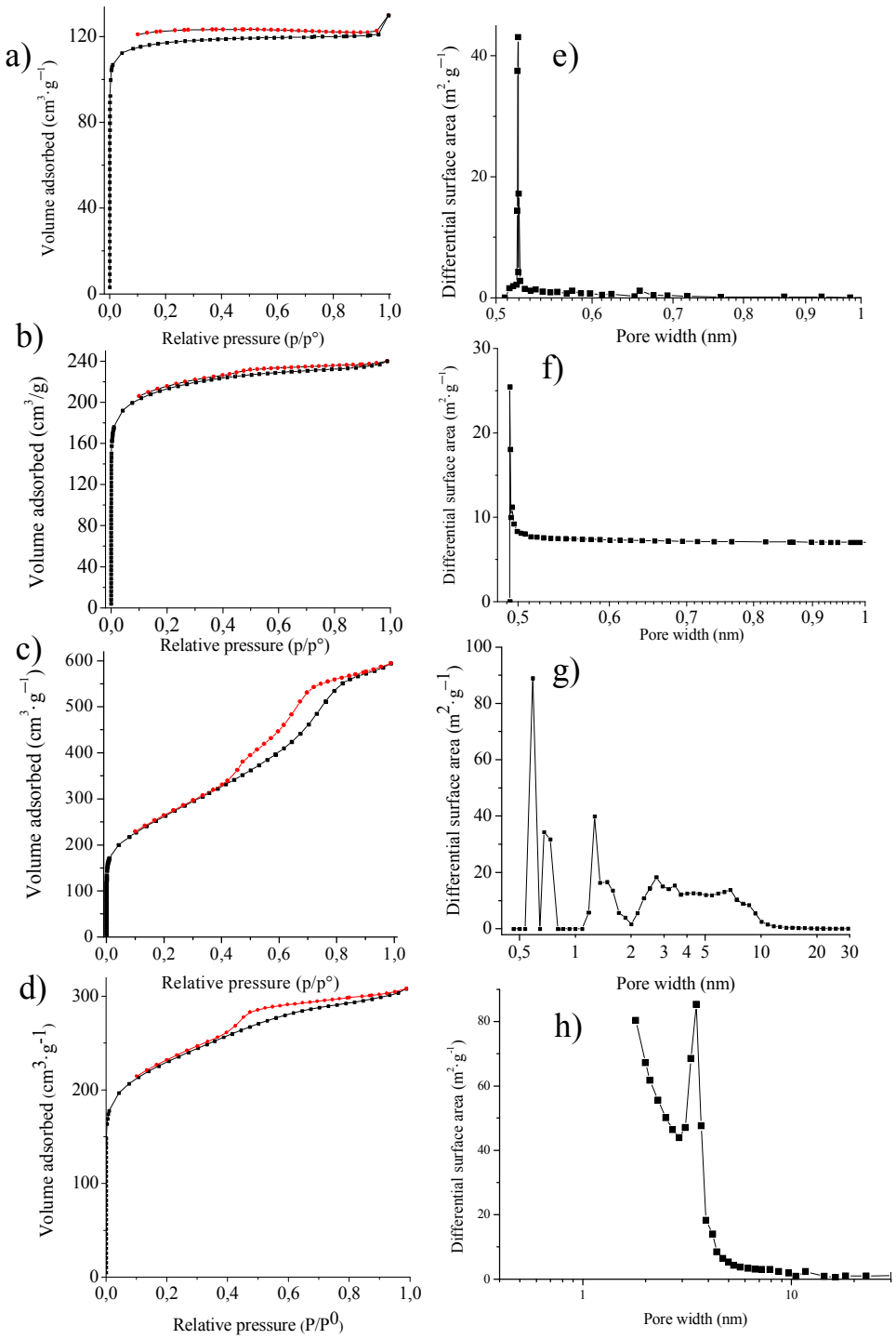

Figure S1. Nitrogen sorption isotherms of carbon foams and pore sizes distribution. a,e) 80HF, b,f) 25HF, c,g) 4F5HF, d,h) 2P5HF.